Enhanced tunability of thermodynamic stability of complex hydrides by the incorporation of H– anions

Shigeyuki Takagi, Terry D. Humphries, Kazutoshi Miwa, and Shin-ichi Orimo

---

Articles you may be interested in

Simultaneous desorption behavior of M borohydrides and Mg2FeH6 reactive hydride composites (M = Mg, then Li, Na, K, Ca)
Appl. Phys. Lett. **107**, 073905 (2015); 10.1063/1.4929340

Ab initio molecular dynamics study of the hydrogen diffusion in sodium and lithium hydrides
J. Appl. Phys. **106**, 016104 (2009); 10.1063/1.3159896

Dehydrogenation from 3 d -transition-metal-doped Na Al H 4 : Prediction of catalysts
Appl. Phys. Lett. **90**, 141904 (2007); 10.1063/1.2719244

Direct formation of Na 3 Al H 6 by mechanical milling Na H ∕ Al with Ti F 3
Appl. Phys. Lett. **87**, 071911 (2005); 10.1063/1.2001756

Density functional study of endohedral complexes M@C 60 (M=Li , Na, K, Be, Mg, Ca, La, B, Al): Electronic properties, ionization potentials, and electron affinities
J. Chem. Phys. **108**, 3498 (1998); 10.1063/1.475783

Enhanced tunability of thermodynamic stability of complex hydrides by the incorporation of H⁻ anions

Shigeyuki Takagi,[1] Terry D. Humphries,[2] Kazutoshi Miwa,[3] and Shin-ichi Orimo[1,2,a]

[1]*Institute for Materials Research, Tohoku University, Sendai 980-8577, Japan*
[2]*WPI-Advanced Institute for Materials Research, Tohoku University, Sendai 980-8577, Japan*
[3]*Toyota Central R&D Laboratories, Inc., Nagakute 480-1192, Japan*

First-principles calculations were employed to investigate hypothetical complex hydrides $(M, M')_4 FeH_8$ ($M = $ Na, Li; $M' = $ Mg, Zn, Y, Al). Besides complex anion $[FeH_6]^{4-}$, these materials contain two H⁻ anions, which raise the total anionic charge state from tetravalent to hexavalent, and thereby significantly increasing the number of combinations of countercations. We have determined that similar to complex hydrides $(M, M')_2 FeH_6$ containing only $[FeH_6]^{4-}$, the thermodynamic stability is tuned by the average cation electronegativity. Thus, the chemical flexibility provided by incorporating H⁻ enhances the tunability of thermodynamic stability, which will be beneficial in obtaining optimal stability for hydrogen storage materials. © *2014 AIP Publishing LLC*. [http://dx.doi.org/10.1063/1.4878775]

The transition metal elements from group 7 to 10 in the periodic table, along with copper and zinc form a variety of complex anions with symmetrically coordinating hydrogen atoms.[1] These anions form ionic bonds with the countercations, yielding a diverse set of complex hydrides.[2] These compounds have attracted attention due to their high hydrogen capacity, which is of practical interest as potential hydrogen storage materials, and much has been learned over the last several decades.[1–11]

A prototypical member of this family is the complex hydride Mg_2FeH_6 composed of abundant elements.[3] This hydride has a high gravimetric hydrogen density of 5.5 mass% and shows reversible hydrogen release/uptake, but its high thermodynamic stability makes room temperature applications challenging.[1,3,4] In this regard, we recently reported a linear correlation between the standard heat of formation and valency-averaged cation electronegativity for the $(M, M')_2 FeH_6$ system,[5] which is based on the idea that the valence states are stabilized by the charge transfer from the electropositive cations to the complex anion. This correlation is useful for tuning stability by selecting the cations with the appropriate electronegativity, as has been reported in borohydrides.[12,13]

The octahedral FeH_6 unit contained in Mg_2FeH_6 takes a tetravalent state, following the 18-electron rule, and thus, every possible combination of countercations is limited to four-fold, i.e., $M^+M'^+M''^+M'''^+$, $M^{2+}M'^+M''^+$, $M^{3+}M'^+$, $M^{2+}M'^{2+}$. One way of increasing these combinations is to raise the anionic charge state. To this end, we have previously reported first-principles calculations for the possibility of forming a hexavalent $[CrH_6]^{6-}$ anion in Y_2CrH_6.[6]

In this Letter, we have employed first-principles calculations based on density functional theory (DFT) to examine the thermodynamic stability of the hypothetical complex hydrides $(M, M')_4 FeH_8$ ($M = $ Na, Li; $M' = $ Mg, Zn, Y, Al) that contain a tetravalent $[FeH_6]^{4-}$ and two H⁻ anions. One

motivation for this study is to provide an alternative method to increase the combinations of countercations by incorporating H⁻ in complex hydrides. The resulting hexavalent anionic charge state significantly increases the number of combinations to more than twice that of the complex hydrides $(M, M')_2 FeH_6$ containing only $[FeH_6]^{4-}$. Supposing that the thermodynamic stability of $(M, M')_4 FeH_8$ is tuned by the average cation electronegativity, similar to the $(M, M')_2 FeH_6$ system, the chemical flexibility provided by incorporating H⁻ should enhance the tunability of thermodynamic stability; this would be highly beneficial in obtaining optimal stability for hydrogen storage. Chemical flexibility is also useful for drastically increasing hydrogen capacity, e.g., the gravimetric hydrogen density of the hypothetical Li_3AlFeH_8 reaches 7.2 mass%, which is approximately 30% higher than that of Mg_2FeH_6 and would be the highest reported density for a complex transition metal hydrides (cf. 6.7 mass% for Li_4FeH_6[14]).

We initially started with a structure determination of the hypothetical $Na_2Mg_2FeH_8$. We first assumed that $Na_2Mg_2FeH_8$ crystallizes in a structure similar to the existing complex hydride $Na_2Mg_2NiH_6$,[7,8] which contains a tetravalent complex ($[NiH_4]^{4-}$) and two H⁻ anions similar to the target material. Then, we replaced the complex anion with an FeH_6 unit, and both the internal atomic coordinates and lattice parameters were relaxed. After relaxation, a phonon calculation was performed to determine whether the relaxed structure was at the true minimum. If the imaginary phonon frequencies were observed, we slightly displaced the atoms along the directions of eigenvectors of the imaginary modes and further relaxed the structure to eliminate them. This procedure was carried out until the ground state was reached. For other compositions, relaxation was started from a structure replacing the Na and Mg in the obtained $Na_2Mg_2FeH_8$ structure with the desired cations.

Calculations were conducted using a plane-wave basis and projector augmented wave method[15,16] within the
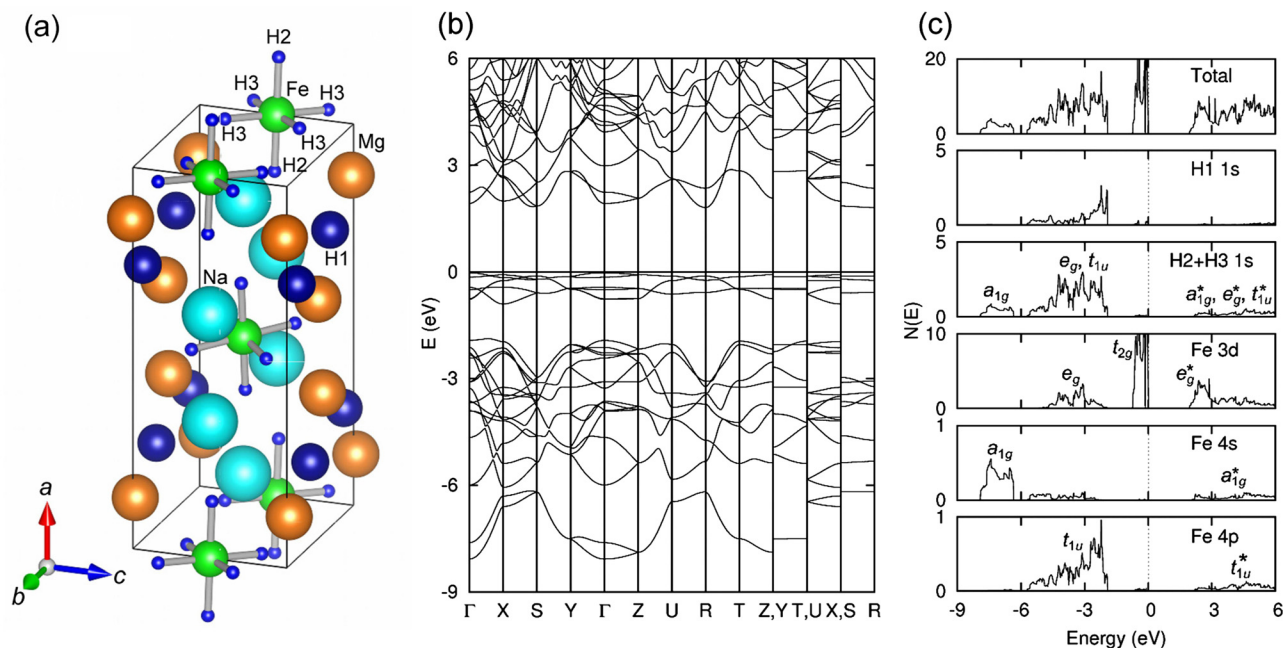
a)Electronic mail: orimo@imr.tohoku.ac.jp

FIG. 1. (a) Crystal structure of $Na_2Mg_2FeH_8$. Na atoms are shown by large (light-blue), Mg by medium (orange), Fe by smaller medium (light-green), and H by small and large (blue) spheres. (b) Electronic band structure, and (c) total electronic DOS, H $1s$, Fe $3d$, Fe $4s$, and Fe $4p$ projections of the 26-atom cell of $Na_2Mg_2FeH_8$, respectively. The energy zero is set at the valence-band maximum.

generalized gradient approximation of Perdew, Burke, and Ernzerhof,[17] as implemented in Vienna *Ab-Initio* Simulation Package (VASP).[18,19] Well-converged plane-wave basis sets were employed with cutoff energies of 600 and 5400 eV for the wavefunctions and charge density, respectively. A $6 \times 6 \times 2$ grid was used for the k-point sampling of the Brillouin zone. The finite-temperature effect and zero-point energy contribution were estimated using the PHONOPY code[20] based on a supercell approach with force constants obtained from VASP calculations. We used a $2 \times 2 \times 2$ supercell (208 atoms), in which cutoff energies of 600 and 5400 eV for the wavefunction and charge density, respectively, and a $2 \times 2 \times 1$ k-point mesh were employed.

Figure 1(a) illustrates the crystal structure of $Na_2Mg_2FeH_8$. The compound preserves the octahedral FeH_6 unit and isolated hydrogen atoms even after the relaxation. Figure 1(a) was produced using the VESTA program (Ref. 23). In comparison with $Na_2Mg_2NiH_6$, a translational symmetry along c-axis occurs, probably reflecting the higher point-group symmetry of the octahedral FeH_6 unit (O_h) relative to the tetrahedral NiH_4 unit (T_d), and thus the unit cell size can be reduced by half (26 atoms, $Z = 2$). The structural properties are summarized in Table I.

Using the relaxed $Na_2Mg_2FeH_8$ structure, we performed structure relaxations of the series of $(M, M')_4FeH_8$. $Li_2Mg_2FeH_8$, $Li_2Zn_2FeH_8$, and Li_3AlFeH_8 crystallize in monoclinic structures, while $Na_2Zn_2FeH_8$, Na_3YFeH_8, and Na_3AlFeH_8 possess the same crystal system as $Na_2Mg_2FeH_8$. A significant difference from the $Na_2Mg_2FeH_8$ structure was found in Li_3YFeH_8, where the unit cell can crystallographically be taken as a triclinic structure and was reduced by half (13 atoms, $Z = 1$), but we continued to use the 26-atom cell in calculations. In any case, the octahedral FeH_6 unit and isolated H atoms coexist in all the relaxed structures. The crystal structure data are summarized in Table II, and detailed structural properties are given in the supplementary material.[21]

Figures 1(b) and 1(c) show the electronic band structure, total density of states (DOS), and H $1s$, Fe $3d$, Fe $4s$, and Fe $4p$ projections for $Na_2Mg_2FeH_8$. We checked for, but did not find any magnetic ordering in this compound. As explained below, the most important feature of the electronic structure is the presence of two distinct H states.

Before discussing the calculated electronic structure, we summarize the expected basic features on the basis of ligand-field theory. In the octahedral O_h point-group symmetry of ligands, the six $1s$ states of H2 and H3 contained in the FeH_6 octahedra (hereafter referred to as H2 + H3) form a symmetry-adapted linear combination (SALC) of a_{1g}, e_g, and t_{1u}, while the Fe $3d$, $4s$, and $4p$ states decompose into t_{2g} and e_g, a_{1g}, and t_{1u} symmetry states, respectively. They hybridize with each other, forming six bonding a_{1g}, e_g, and t_{1u}, three nonbonding t_{2g}, and six antibonding $a_{1g}^\star$, $e_g^\star$, and $t_{1u}^\star$ symmetry states. In contrast, the $1s$ states of isolated H1 are expected to show much less hybridization with Fe states due to the absence of ligand-field effects. Given the higher electronegativity of H than that of Fe, the H1 $1s$ states would appear far below the Fe $3d$ derived nonbonding t_{2g} states. Since the total electron count of $Na_2Mg_2FeH_8$ is 22 (44 per unit cell), the six

TABLE I. Structural properties of $Na_2Mg_2FeH_8$ with *Pbam* (No. 55) space group symmetry ($a = 11.018$ Å, $b = 5.302$ Å, and $c = 4.451$ Å).

Atom	Wyckoff notation	x	y	z
Fe	$2b$	0	0	1/2
Na	$4h$	0.3594	−0.0004	1/2
Mg	$4g$	0.3713	0.4646	0
H1	$4g$	0.2796	0.1487	0
H2	$4h$	0.8558	0.0310	1/2
H3	$8i$	0.0111	0.2160	0.2576

TABLE II. List of $(M, M')_4$FeH$_8$ with their gravimetric hydrogen densities ρ_m (in mass%), crystal structure data (lattice parameters in Å and degrees), average cation electronegativities χ_{AR}, and standard heats of formation ΔH_{form} (in kJ/mol).

Composition	ρ_m	Z	Crystal system	Space group	a	b	c	α	β	γ	χ_{AR}	ΔH_{form}
Na$_2$Mg$_2$FeH$_8$	5.1	2	Orthorhombic	$Pbam$ (55)	11.018	5.302	4.451	90	90	90	1.16	-328.3
Li$_2$Mg$_2$FeH$_8$	6.4	2	Monoclinic	$P2_1/c$ (14)	4.430	4.700	10.465	90	89.254	90	1.14	-373.2
Na$_2$Zn$_2$FeH$_8$	3.4	2	Orthorhombic	$Pmna$ (53)	5.186	4.325	10.897	90	90	90	1.44	-122.2
Li$_2$Zn$_2$FeH$_8$	3.9	2	Monoclinic	$P2_1/c$ (14)	4.427	4.772	9.594	90	90.746	90	1.43	-170.4
Na$_3$YFeH$_8$	3.6	2	Orthorhombic	$Amm2$ (38)	4.801	4.960	12.516	90	90	90	1.06	-398.1
Li$_3$YFeH$_8$	4.6	1	Triclinic	$P1$ (1)	6.251	4.484	4.647	90.184	88.631	69.376	1.04	-485.0
Na$_3$AlFeH$_8$	5.0	2	Orthorhombic	$Pmc2_1$ (26)	4.429	5.292	11.245	90	90	90	1.24	-264.8
Li$_3$AlFeH$_8$	7.2	2	Monoclinic	$P2_1$ (4)	4.279	9.737	4.739	90	90.063	90	1.22	-369.4

bonding a_{1g}, e_g, and t_{1u} (twelve states per unit cell), three non-bonding t_{2g} (six states per unit cell), and two H1 $1s$ states (four states per unit cell) will be fully occupied, and the Fermi level will fall in the gap between the nonbonding t_{2g} and anti-bonding $e_g^\star$ states. Thus H1 holds an additional electron and forms the H$^-$ anion, while H2 and H3 form covalent bonds with Fe. These bonding features are clearly seen in the calculated electronic structure in Figs. 1(b) and 1(c).

The two lowest bands from -7.9 to -6.3 eV are regarded as the a_{1g} states, as is evident from the strong mixing of H2 + H3 $1s$ and Fe $4s$ states that can be clearly seen in the corresponding projections. A manifold of 14 bands extending from -6 to -1.9 eV can be understood as a mixture of e_g, t_{1u}, and H1 $1s$ states; while there are noticeable

cross-gap hybridizations of the H2 + H3 $1s$ states with the Fe $3d$ and $4p$ states, as may be seen both from the Fe character in the valence bands and the H2 + H3 $1s$ character in the conduction bands, the contribution from H1 $1s$ states can only be seen in the valence states. The Fe $3d$ states give rise to the DOS peak just below the Fermi level, which is assigned to be t_{2g} states due to the absence of any H character. The contributions to the valence bands from Na and Mg states are negligible, and they are not shown here.

To summarize the results so far, the valence bands of Na$_2$Mg$_2$FeH$_8$ include the bonding a_{1g}, e_g, and t_{1u}, non-bonding t_{2g}, and $1s$ states of isolated H1 and consist of eleven bands filled with 22 electrons per formula unit. Thus, while the H2 and H3 atoms form covalent bonds with Fe, the isolated H1 atoms exist as H$^-$ anions; the two distinct H states are clearly distinguishable in the electronic structure. The electropositive Na and Mg donate a total of six electrons per formula unit to the FeH$_6$ octahedron and isolated H1, taking the hexavalent state.

A similar bonding feature related to H is found in other compositions of $(M, M')_4$FeH$_8$. Figure 2 shows the H $1s$ and Zn $3d$ projections of $(M, M')_4$FeH$_8$. The electronic structures of all the compounds, except those containing Zn, evidently show the low-lying a_{1g} states followed by the mixture of e_g, t_{1u}, and H1 $1s$ states. For the Zn-containing compounds,
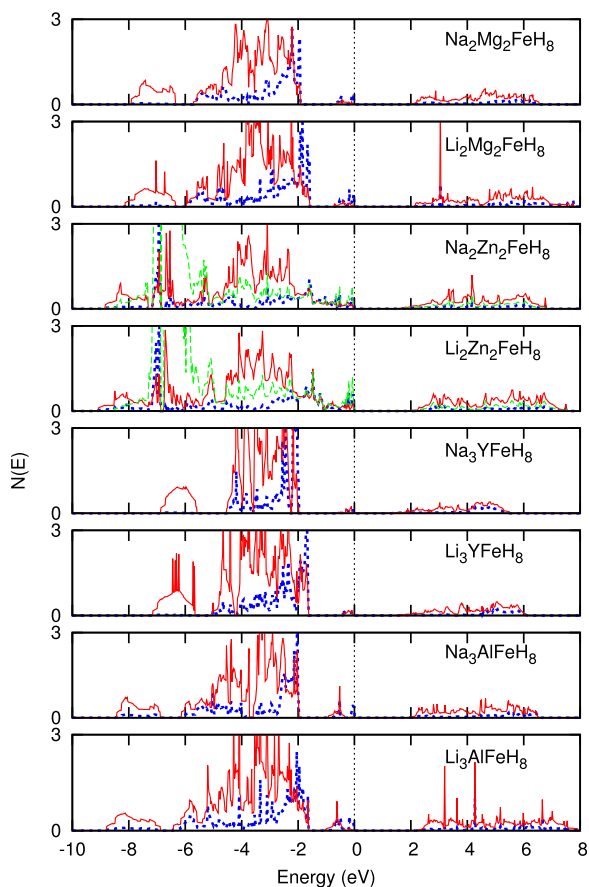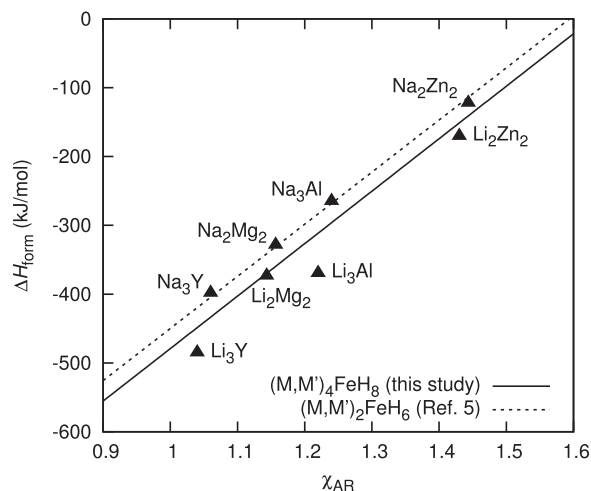

FIG. 2. H $1s$ and Zn $3d$ projections of $(M, M')_4$FeH$_8$. (Red) Solid lines indicate the projection onto the octahedrally coordinating H2 and H3 atoms, (blue) dotted lines denote the projection onto the isolated H1 atoms, and (light-green) dashed lines are the Zn $3d$ projection. The energy zero is set at the valence-band maximum.

FIG. 3. Standard heat of formation ΔH_{form} (in kJ/mol), as a function of average cation electronegativity on the Allred–Rochow scale χ_{AR} for $(M, M')_4$FeH$_8$. Solid line is a least-squares fit to the results in this study (Eq. (1)). As a reference, dotted line denotes the fit to the results for $(M, M')_2$FeH$_6$ reported in Ref. 5.

$Li_2Zn_2FeH_8$ and $Na_2Zn_2FeH_8$, the low-lying Zn $3d$ states give rise to the DOS peak centered at approximately -6.3 eV, and modestly hybridize with the $1s$ states of both H1 and H2 + H3 below the Fermi level. These are mixing of occupied states and as such do not signify chemical bonding. There is little contribution of Zn $4sp$ states to the valence bands (not shown here), and thus, the Zn atoms exist as divalent cations. In any case, all these materials are complex hydrides with incorporated H^- anions and take the hexavalent anionic state.

Finally, we discuss the thermodynamic stability of the complex transition metal hydrides $(M, M')_4FeH_8$ in a similar manner to Ref. 5. The standard heats of formation ΔH_{form} were evaluated from the total energy calculations with incorporation of finite-temperature effect and zero-point energy contribution within the harmonic approximation (Table II). We used the Allred–Rochow scale[22] to estimate the valence-averaged cation electronegativities, χ_{AR}.

Figure 3 shows a definite correlation between the standard heat of formation and average cation electronegativity for $(M, M')_4FeH_8$. Assuming a linear dependence of the heats of formation on the electronegativities, a least-squares fit to the results yields

$$\Delta H_{form} = 762.6\chi_{AR} - 1241.7, \tag{1}$$

with an absolute mean error of 29.2 kJ/mol. Interestingly, Eq. (1) agrees well with that reported for $(M, M')_2FeH_6$, $\Delta H_{form} = 757.5\chi_{AR} - 1207.4$,[5] with deviations of 0.67% and 2.84% in the gradient and y-intercept, respectively. This implies that the correlation is quite general with or without the incorporation of H^-. In this context, one may expect that the correlation will also be true for the complex transition metal hydrides with more than two H^- anions; this should provide much greater chemical flexibility, leading to further tunability of thermodynamic stability. Although Ref. 5 reports that Zn_2FeH_6 is not thermodynamically stable since it has a positive heat of formation of 50.5 kJ/mol, the corresponding complex hydrides $Na_2Zn_2FeH_8$ and $Li_2Zn_2FeH_8$ incorporating H^- show negative heats of formation of -122.2 and -373.2 kJ/mol, respectively. This exemplifies the enhanced tunability achieved by the incorporation of H^- anions into complex hydrides.

In conclusion, first-principles calculations on the hypothetical complex hydrides $(M, M')_4FeH_8$ indicate that their standard heat of formation can be tuned by altering the average cation electronegativity. These materials have two incorporated H^- anions, which significantly increase the possible number of combinations of countercations. The resulting chemical flexibility implies an enhanced tunability of thermodynamic stability that will become vital whilst designing materials with thermodynamic stability suitable for hydrogen storage applications.

[1]K. Yvon, Chimia **52**, 613 (1998).
[2]W. Bronger, Angew. Chem., Int. Ed. Engl. **30**, 759 (1991).
[3]J. J. Didisheim, P. Zolliker, K. Yvon, P. Fischer, J. Shefer, M. Gubelmann, and A. F. Williams, Inorg. Chem. **23**, 1953 (1984).
[4]B. Bogdanovic, A. Reiser, K. Schlichte, B. Spliethoff, and B. Tesche, J. Alloys Compd. **345**, 77 (2002).
[5]K. Miwa, S. Takagi, M. Matsuo, and S. Orimo, J. Phys. Chem. C **117**, 8014 (2013).
[6]S. Takagi, K. Miwa, T. Ikeshoji, R. Sato, M. Matsuo, G. Li, K. Aoki, and S. Orimo, J. Alloys Compd. **580**, S274 (2013).
[7]K. Kadir and D. Noréus, Inorg. Chem. **46**, 2220 (2007).
[8]M. Orlova, J.-P. Rapin, and K. Yvon, Inorg. Chem. **48**, 5052 (2009).
[9]S. Takagi, K. Miwa, T. Ikeshoji, M. Matsuo, M. Kano, and S. Orimo, Appl. Phys. Lett. **100**, 021908 (2012).
[10]M. Matsuo, H. Saitoh, A. Machida, R. Sato, S. Takagi, K. Miwa, T. Watanuki, Y. Katayama, K. Aoki, and S. Orimo, RSC Adv. **3**, 1013 (2013).
[11]S. Takagi, T. Ikeshoji, M. Matsuo, T. Sato, H. Saitoh, K. Aoki, and S. Orimo, Appl. Phys. Lett. **103**, 113903 (2013).
[12]Y. Nakamori, K. Miwa, A. Ninomiya, H. Li, N. Ohba, S. Towata, A. Züttel, and S. Orimo, Phys. Rev. B **74**, 045126 (2006).
[13]S. Orimo, Y. Nakamori, J. R. Eliseo, A. Züttel, and C. M. Jensen, Chem. Rev. **107**, 4111 (2007).
[14]S. Takagi, T. Ikeshoji, T. Sato, K. Aoki, and S. Orimo, J. Jpn Inst. Met. Mater. **77**, 604 (2013).
[15]P. E. Blöchl, Phys. Rev. B **50**, 17953 (1994).
[16]G. Kresse and D. Joubert, Phys. Rev. B **59**, 1758 (1999).
[17]J. P. Perdew, K. Burke, and M. Ernzerhof, Phys. Rev. Lett. **77**, 3865 (1996).
[18]G. Kresse and J. Hafner, Phys. Rev. B **47**, 558 (1993).
[19]G. Kresse and J. Furthmüller, Phys. Rev. B **54**, 11169 (1996).
[20]A. Togo, F. Oba, and I. Tanaka, Phys. Rev. B **78**, 134106 (2008).
[21]See supplementary material at http://dx.doi.org/10.1063/1.4878775 for the detailed structural properties of $(M, M')_4FeH_8$.
[22]A. L. Allred and E. G. Rochow, J. Inorg. Nucl. Chem. **5**, 264 (1958).
[23]K. Momma and F. Izumi, J. Appl. Cryst. **44**, 1272 (2011).